frontiers in Immunology

ORIGINAL RESEARCH
published: 30 October 2020
doi: 10.3389/fimmu.2020.584229

Endothelial Basement Membrane Laminins as an Environmental Cue in Monocyte Differentiation to Macrophages

Lixia Li[1,2†], *Jian Song*[1,2†], *Omar Chuquisana*[1,2], *Melanie-Jane Hannocks*[1,2], *Sophie Loismann*[1,2], *Thomas Vogl*[2,3], *Johannes Roth*[2,3], *Rupert Hallmann*[1,2] *and Lydia Sorokin*[1,2*]

[1] Institute of Physiological Chemistry and Pathobiochemistry, University of Muenster, Muenster, Germany, [2] Cells-in-Motion Interfaculty Centre, University of Muenster, Muenster, Germany, [3] Institute of Immunology, University of Muenster, Muenster, Germany

OPEN ACCESS

Edited by:
Deirdre R. Coombe,
Curtin University, Australia

Reviewed by:
Beat A. Imhof,
Université de Genève, Switzerland
Leo Marc Carlin,
University of Glasgow,
United Kingdom

***Correspondence:**
Lydia Sorokin
sorokin@uni-muenster.de

[†]These authors have contributed equally to this work

Specialty section:
This article was submitted to Inflammation, a section of the journal Frontiers in Immunology

Received: 16 July 2020
Accepted: 08 October 2020
Published: 30 October 2020

Citation:
Li L, Song J, Chuquisana O, Hannocks M-J, Loismann S, Vogl T, Roth J, Hallmann R and Sorokin L (2020) Endothelial Basement Membrane Laminins as an Environmental Cue in Monocyte Differentiation to Macrophages. Front. Immunol. 11:584229. doi: 10.3389/fimmu.2020.584229

Monocyte differentiation to macrophages is triggered by migration across the endothelial barrier, which is constituted by both endothelial cells and their underlying basement membrane. We address here the role of the endothelial basement membrane laminins (laminins 411 and 511) in this monocyte to macrophage switch. Chimeric mice carrying CX3CR1-GFP bone marrow were employed to track CCL2-induced monocyte extravasation in a cremaster muscle model using intravital microscopy, revealing faster extravasation in mice lacking endothelial laminin 511 (*Tek-cre::Lama5*$^{-/-}$) and slower extravasation in mice lacking laminin 411 (*Lama4*$^{-/-}$). CX3CR1-GFP^{low} extravasating monocytes were found to have a higher motility at laminin 511 low sites and to preferentially exit vessels at these sites. However, *in vitro* experiments reveal that this is not due to effects of laminin 511 on monocyte migration mode nor on the tightness of the endothelial barrier. Rather, using an intestinal macrophage replenishment model and *in vitro* differentiation studies, we demonstrate that laminin 511, together with the attached endothelium, promote monocyte differentiation to macrophages. Macrophage differentiation is associated with a change in integrin profile, permitting differentiating macrophages to distinguish between laminin 511 high and low areas and to preferentially migrate across laminin 511 low sites. These studies highlight the endothelial basement membrane as a critical site for monocyte differentiation to macrophages, which may be relevant to the differentiation of other cells at vascular niches.

Keywords: monocyte, macrophage, endothelial basement membrane, laminin, intravital microscopy

INTRODUCTION

Monocytes are a diverse population that varies in origin, *in vivo* localization, and function. They represent an important early line of defense against infectious agents or reaction to tissue damage and in several tissues bone marrow derived monocytes play a critical role in the replenishment of resident monocytes, macrophages, and dendritic cells (DCs) required for tissue immunity (1).

Trafficking and extravasation are, therefore, critical to their function. There are at least two subsets of monocyte populations, Ly6C^{high}CCR2^{high}CX3CR1^{low} inflammatory monocytes that extravasate into tissues under both sterile and infectious inflammatory conditions, and patrolling monocytes that are Ly6C^{low}CCR2^{low}CX3CR1^{high} (2, 3). However, data suggest that a continuum of monocyte phenotypes occur *in vivo* that are modulated by tissue/environmental factors (4). Several studies have demonstrated that the endothelium plays a role in the switch to macrophages (1, 5); whether the underlying endothelial basement membrane also contributes to this step has not been considered to date.

Our previous work has shown that the basement membrane of vascular endothelium affects leukocyte extravasation by influencing adhesion and migration of extravasating cells (6, 7), and by affecting the tightness of endothelial monolayer (8). Laminins were identified as the effector molecules in endothelial basement membranes, with laminin 511 (composed of α5, β1, γ1 chains) playing a decisive role. Endothelial basement membranes of arteries, arterioles and capillaries typically show high expression of the two main endothelial laminins, laminin 411 and 511, with progressively less laminin 511 occurring in the postcapillary venules, venules and veins resulting in patches of laminin 411 positive and laminin 511 low expression which define the preferred sites of leukocyte extravasation (6, 7, 9). Although limited, data suggest that laminin 511 affects extravasation of different leukocyte types in different manners; while T cell migration is inhibited by direct interaction with laminin 511 (7), neutrophils can migrate across this substrate *in vitro* and their avoidance of laminin 511 high sites *in vivo* rather correlates with the higher endothelial-to-endothelial cell junctional adhesion strength at these sites (8). Recent intravital imaging of sterile inflammation in the cremaster muscle also revealed that extravasating myeloid cells spend disproportionately long periods of time at the interface between the endothelial monolayer and the endothelial basement membrane and in breaching the basement membrane compared to their rapid penetration of the endothelial monolayer (8), suggesting that the subendothelial compartment may be a site of reprogramming required for subsequent steps (10).

Macrophages have been shown to bind and migrate on laminin *in vitro* (11). While the laminin isoform employed in these studies does not occur in endothelial basement membranes, it shares similarities with endothelial laminin 511 and the receptors identified to be involved in macrophage-laminin interactions also recognize the endothelial laminin isoforms (12). Macrophages, however, are not likely to extravasate across an endothelial basement membrane *in vivo*, rather they are the consequence of monocyte extravasation or constitute a tissue resident population that forms during development. Due to the difficulty in obtaining sufficient numbers of monocytes for *in vitro* analyses, there is a paucity of information on monocyte-extracellular matrix interactions relevant to the extravasation process (13). We, therefore, here use live imaging of CCL-2 induced monocyte extravasation in the cremaster muscle model to investigate whether the endothelial basement membrane represents an environmental factor that affects monocyte phenotype and/or infiltration into tissues. Chimeric mice carrying CX3CR1-GFP bone marrow are used to track extravasating monocytic cells in WT host mice and in mice lacking the main endothelial basement membrane laminins, laminin 411 (*Lama4*$^{-/-}$) and laminin 511 (*Tek-cre::Lama5*$^{-/-}$). As reported for other leukocyte types, monocyte extravasation occurred preferentially at laminin 511 low sites; however, *in vitro* experiments revealed that this was not due to direct effects of laminin 511 on migration modes, nor effects on the tightness of the endothelial monolayer. Rather, using an intestinal macrophage replenishment model, we demonstrate that laminin 511 together with the attached endothelium provide a decisive cue, promoting monocyte differentiation to macrophages which, in turn, affects the extent of tissue infiltration.

MATERIALS AND METHODS

Mice

Wild-type (WT) C57BL/6, laminin α4 knockout mice (*Lama4*$^{-/-}$) (14), endothelial specific laminin α5 knockout mice (*Tek-cre::Lama5*$^{-/-}$) (15, 16), and CX3CR1$^{GFP/+}$ mice (17) were employed. Equal proportions of male and female mice were employed and no difference were noted between sexes. Animals were held in controlled temperature, humidity and day/night cycles; female and pre-mating male mice were maintained in groups of a maximum of 5 animals/IIL cage, post-mating males were maintained in separate cages. All animal experiments were performed according to German Animal Welfare guidelines.

Bone Marrow Chimera Generation

Recipient *Lama4*$^{-/-}$ and *Tek-cre::Lama5*$^{-/-}$ mice and their corresponding WT littermates were lethally irradiated at 15 Gy. 10^7 bone marrow cells from femurs and tibias of CX3CR1$^{GFP/+}$ mice were intravenously (i.v.) injected into each irradiated mouse. Reconstitution efficiency was analyzed at 6 weeks for CD45$^+$GFP$^+$ versus CD45$^+$GFP$^-$ cells, or using the polymorphic lineage determinants (CD45.1 or CD45.2), for tracking GFP$^+$ CD45.1$^+$ donor cells in CD45.2 hosts. Only mice with >95% donor cell engraftments were employed for intravital microscopic imaging.

Cells

Human umbilical venular endothelial cells (HUVECs) were cultured in endothelial cell growth medium (Promo Cell) at 37°C and 5% CO_2 and used up to passage 5. Endothelioma cell lines were generated from *Lama4*$^{-/-}$ embryos (eEND4.1) and WT littermates (eENDwt) as described previously (18); presence or absence of *Lama4* was checked by PCR and laminin α5 protein was quantified by Western blot. All endothelioma cell lines were cultured in DMEM plus 10% fetal calf serum (FCS) at 37°C and 5% CO_2.

Murine Hoxb8 is a myeloid progenitor cell line that can be differentiated to monocytes or macrophages upon removal of β-estradiol (Sigma-Aldrich) (19). Hoxb8 progenitor cell lines were generated from CD18$^{-/-}$ C57BL/6 mice and their WT littermates (20) and were cultured in RPMI 1640 containing 10% FCS, 40ng/ml GM-CSF (Promokine) and 1 μM β-estradiol.

Differentiation to monocyte-like Hoxb8 cells was induced by removal of β-estradiol from the culture medium for 3 days (19).

Bone marrow was flushed from tibias and femurs of WT C57BL/6 or $CD18^{-/-}$ mice, sieved through a 70-μm sieve and red blood cells were lysed. The cells were pelleted and resuspended in DMEM with 10% FCS. The cells were incubated for 24 h at 37°C and 5% CO_2 on bacterial plates, non-adherent cells were then harvested, transferred to a new bacterial plate in DMEM plus 10% FCS supplemented with 20 ng/ml M-CSF (Promokine) and cultured for 8 days to generate bone marrow derived macrophages (BMDMs).

Human monocytes were isolated from buffy coats of blood from healthy donors. A two-step procedure with a single gradient in each step was used, which included centrifugation through a Pancoll gradient (Pan-Biotech) (density = 1.070 g/ml) followed by a Percoll (General Electric Company) gradient (density = 1.064 g/ml). Monocyte purity was >85% as defined by flow cytometry for CD14 antibody (M5E2, Biolegend). Monocytes were cultured overnight in McCoy's medium (Sigma-Aldrich) plus 15% FCS at 37°C and 7% CO_2 in Teflon cell culture bags (OriGen) prior to use.

Intravital Microscopy

Mice were anesthetized using intra peritoneal (i.p.) injection of a mixture of ketamine hydrochloride (125 mg/kg; Sanofi Winthrop Pharmaceuticals) and xylazine (12.5 mg/kg; TranquiVed, Phoenix Scientific) in saline. Intra-scrotal injection of 500 ng CCL2 (Biolegend) in 0.2 ml saline 3.5 or 1.5 h before cremaster muscle exteriorization was employed to specifically induce monocyte extravasation. Intravital microscopy was performed using an Axioscope A1 microscope equipped with an immersion objective (SW 40/0.75 NA) and stroboscopic epifluorescent illumination (Colibri 2, Zeiss), as described previously (8). Blood flow center-line velocity was determined by imaging fluorescent beads (0.5μm, Polysciences) injected i.v. before image acquisition, which were converted to mean blood flow velocities by multiplying with an empirical factor of 0.625 (21). Recorded images were analyzed using ImageJ software. In some experiments, Alexa 650-labeled anti-laminin α5 (antibody 4G6) was injected intra-scrotally to mark the endothelial basement membrane (8); intravital microscopy was otherwise performed as described above.

To correlate speeds of migration with CX3CR1-GFP expression levels, the ImageJ plugin-TrackMate was used to track the motility of CX3CR1-GFP^{high} patrolling and CX3CR1-GFP^{low} extravasating cells at laminin 511^{high} and laminin 511^{low} areas. CX3CR1-GFP^{high} and CX3CR1-GFP^{low} cells were identified using basic intensity quantification with ImageJ; a MFI above 11000 AU defined CX3CR1-GFP^{high} cells. LoG detector was used to detect the CX3CR1-GFP cells and Simple LAP tracker was used for tracking the cells. For speed analyses, at least 60 frames were selected for each track and the mean speed of the track was calculated.

Experiments were performed at least three times/chimera. In all experiments, three to nine different postcapillary venules were imaged/mouse and analyzed. Experiments were performed using age and sex matched WT chimera and laminin knockout chimeras. Biological replicates were individual animals or chimeras, technical replicates were analyses performed on different postcapillary venules in the same animal.

Confocal Microscopy

After live cell imaging the cremaster muscle was removed, fixed in 1% PFA for 1 h, blocked and permeabilized in PBS containing 5% FCS and 0.5% Triton X-100 for 30 min. Incubations with primary antibodies were performed overnight at 4°C, followed by secondary antibody incubation for 2 h at room temperature. To quantify the proportions of CX3CR1-$GFP^{+}MHCII^{+}$ cells in total GFP^{+} cells, the cremaster muscles were stained by using primary antibodies including rabbit anti-mouse laminin α5 (antibody 405) or anti-mouse laminin α4 (antibody 377) and Brilliant Violet 411–conjugated rat anti-mouse MHC II (Biolegend); monocytes were identified by $CX3CR1^{GFP}$ expression. Alexa 647-anti-rabbit secondary antibodies (Dianova) were employed. 2–7 postcapillary venules were imaged/chimera and the images were analyzed using ImageJ software.

Dynamic *in situ* cytometry was employed to investigate associations between laminin 511 expression and CX3CR1-GFP mean fluorescence intensity (MFI): cremaster muscles were stained with rat anti-mouse PECAM-1 (MEC13.3, BD Bioscience) and rabbit anti-mouse laminin α5 (antibody 405) (6) and monocytes were identified by CX3CR1-GFP expression; Alexa 647–conjugated anti-rat and Alexa 555–conjugated anti-rabbit secondary antibodies (Abcam) were employed. CX3CR1-GFP expression was analyzed with Flowjo v10.4 and the image files were converted into "flow cytometry standard" files for analysis by flow cytometry software. Image pixels were reconstituted relative to locations in the X and Y axes; laminin 511^{high} and laminin 511^{low} regions were gated separately and CX3CR1-GFP MFI were analyzed in these two regions. Data were expressed as percent CX3CR1-GFP^{low} cells of total CX3CR1-GFP positive cells in laminin 511^{high} and laminin 511^{low} regions. These analyses were performed on >5 postcapillary venules in each of 3 mice/chimera.

Adhesion Assay

Cell attachment assays were performed using dot adhesion assays. Twelve-well Nunc Maxisorb plates were coated overnight at 4°C with 5 μl dots of 20 μg/ml laminin 411, laminin 511, VCAM-1 (R&D) or ICAM-1 (R&D), wells were blocked with 1% BSA for 1 h at 37°C and washed with PBS before use. Cells (1×10^6) in adhesion buffer (DMEM, 0.5% BSA, 50 mM HEPES, pH 7.5) were added to coated wells and allowed to adhere for 1 h at 37°C. Non-adherent cells were removed and attached cells were fixed in 4% paraformaldehyde (PFA) for 10 min and stained by 0.5% crystal violet for 10 min. Cells bound to the dots of different substrates were imaged using an inverse Axiovert microscope (Zeiss) and the number of adherent cells per substrate was quantified using ImageJ software. Adhesion assays were carried out using human monocytes and mouse monocyte-like Hoxb8 cells.

Inhibition assays to assess receptors responsible for adhesion to different substrates involved pre-incubation of cells at 4°C for 30 min prior to addition to protein-coated 12-well plates with

20 μg/ml anti-human integrin β2 antibody (TS1/18), anti-human integrin β1 antibody (P5D2) and anti-mouse integrin β3 (antibody 2C9.G2), or 50 μg/ml anti-mouse integrin β1 antibody (Ha2/5) and anti-human and mouse integrin α6 antibody (GoH3). Inhibition assays were performed using 20 μg/ml of extracellular matrix protein.

Biological replicates were different batches of Hoxb8 cells, human monocytes or BMDM preparations used in separate experiments, technical replicates were repetitions of the same test (e.g., adhesion on a specific laminin isoform) in one experiment.

Migration Assays

Twenty-four–well Transwell inserts (6.5 mm^2) with polycarbonate filters (5-μm pore size) (Corning Costar) were used for transmigration assays. Membranes were coated overnight at 4°C with 10 μg/ml laminins 411 or 511 and blocked with 1% BSA in PBS for 1 h at 37°C. Human monocytes, mouse Hoxb8 monocytes and BMDM were used in transmigration assays. Cells (5×10^5) in 100 μl adhesion buffer were added to the upper chamber and either 500 ng/ml CCL2 (R&D Systems) or 10 nM C5a (R&D Systems) was added to the bottom chamber. Cells were permitted to transmigrate at 37°C for 4 h, and the number of transmigrated cells was expressed as a percentage of the total cells initially added. For trans-endothelial migration, HUVEC or bEND.5 cells were plated at confluent densities onto the laminin 411, 511, or 111 coated filters and stimulated for 4 h with 5 nM tumor necrosis factor-α (TNF-α; R&D Systems), then human monocytes or monocyte Hoxb8 cells were added. These experiments were repeated three times with triplicates/experiment.

Two-dimensional Chemotaxis assays utilized the Ibidi μ-Slide Chemotaxis system and 20 nM C5a as chemoattractant. Slides were coated overnight at 4°C with 10 μg/ml laminin 411 or 511, and mouse WT or $CD18^{-/-}$ lipopolysaccharide (LPS/1 μg/ml) (Sigma) activated BMDM cells (1×10^6 cells/ml) were added in attachment buffer (RPMI 1640 medium, 20 mM Hepes, 10% FCS) and monitored by time-lapse video microscopy every 2 min for 24 h. Cell migration tracks between 6 and 12 h were analyzed by ImageJ using a manual tracking plugin and the Ibidi software chemotaxis and migration tool. A minimum of 20 randomly selected cells on each substrate were manually tracked and cell velocities were measured/experiment. The experiment was repeated three times.

Isolation of Colonic Lamina Propria Cells

LP cells were purified from colons of adult (8–12 weeks old) and day 21 postnatal (P21) mice by enzymatic digestion (22). Colons were excised and washed in PBS, opened longitudinally and cut into 0.5 cm sections, and shaken vigorously in Hank's balanced salt solution (HBSS) containing 2% FCS. To remove the epithelial layer, 2 mM EDTA in Ca^{2+}/Mg^{2+} free HBSS was added twice with shaking for 15 min each at 37°C. The remaining tissue was incubated in digestion buffer [RPMI 1640, 10% FCS, 1.25 mg/ml collagenase D (Roche), 0.85 mg/ml collagenase V (Sigma-Aldrich), 1 mg Dispase (Gibco), and 30 U/ml DNase (Roche)] for 30–45 min at 37°C with shaking. The resulting cell suspension was passed through a 40 μm cell strainer and washed twice in RPMI 1640. The experiments with adult and P21 mice were done three times with at least two mice/mouse strain/experiment. Typically, 4–5 million single cells were obtained from one adult colon, and approximately 2 million single cells from one P21. Total numbers of cells isolated in adult or P21 colons were the same regardless of genotype.

Flow Cytometry

Colonic LP samples (2 million cells/staining) were stained at 4°C for 20 min with the following antibodies: Ly6C-FITC (AL-21, BD Pharmingen), F4/80-PE (BM8, BioLegend), Siglec F-PE-CF594 (E50-2440, BD Bioscience), Ly6G PE-Cy7 (1A8, BioLegend), CD11b-APC (M1/70, eBioscience), CD11c-AF700 or -APC-R700 (N418, BioLegend), MHCII-BV421 (M5/114.15.2, BioLegend), and CD45-BV510 (30-F11, BioLegend) at 4°C for 20 min. Dead cells were identified by staining with eFluor 780 Fixable Viability dye (eBioscience) and gatings were performed as described previously (22).

For analyses of integrin receptors on human monocytes, mouse Hoxb8 monocytes and mouse BMDMs, antibodies to integrins β1 (mouse 9EG7 (23)/human P5D5) (24), α6 (GoH3, BD Pharmingen), α5 (mouse 5H10-27, BD Pharmingen/human P1D6) (24), α4 (PS/2, Abcam), α3 (mouse polyclonal, R&D/human P1B5) (24), β3 (mouse 2C9.G2, Biolegend/human B3A, Chemicon), and β2 (mouse C71/16, BD Pharmingen/human TS1/18, Thermo Scientific) were employed. Cells were analyzed with a Gallios (Beckman Coulter) or Celesta (BD) flow cytometer and FlowJo software.

In Vitro Monocyte Differentiation

Three-dimensional collagen type I was prepared using eight-parts rat collagen type I (Sigma) and one-part 10× DMEM and was neutralized to pH 7.0–7.5 by adding 0.5 parts 0.5N NaOH; 400 μl collagen I gel was then added immediately to each well of a 24-well plate. Endothelial cells (e.END4.1, e.ENDwt) were seeded onto the collagen type I gel base and were incubated at 37°C overnight. Splenic monocytes were isolated by depleting CD19, Ly6G, CD11c, CD3ε, Siglec-F, MHCII, and CD11c positive cells using magnetic beads (Miltenyi Biotec); 5×10^5 cells were plated onto the confluent endothelial cells for 16 h at 37°C. The conditioned medium was collected for cytokines analyses, and remaining unattached cells were removed by 5× washing with DMEM; 400 μl Collagenase D (2 mg/ml, Sigma) was then added and the cultures digested at 37°C for 30 min. Cells were harvested and analyzed by flow cytometry for PECAM-1, Ly6C, MHCII, CD11b, and F4/80 expression. The same experiments were performed with splenocytes preincubated for 30 min in the presence of 25 μg/ml integrin α6 function blocking antibody (GoH3) or an isotype control. Experiments were performed three times using cells from two mice. Cytokines were measured in 5× concentrated conditioned media using Th1/Th2 10 Plex Flowcytomix Kit (eBioscience).

Statistical Analyses

Data sets were tested for normal distribution with a D`Agostino & Pearson normality test. If all data sets of one experiment

passed the normality test, significance was analyzed with a Welch's t-test. A Mann-Whitney test was applied if the data was not normally distributed. P-values of <0.05 were considered significant.

RESULTS

Monocyte Extravasation in the Cremaster Muscle Model

CX3CR1$^{GFP/+}$ mice have a high GFP expression on monocytes, and while GFP can also be expressed by a subset of dendritic cells (DCs) and NK T cells, the GFP levels on these cells are significantly lower than that on monocytes (17, 25, 26). We therefore transferred bone marrow cells from CX3CR1$^{GFP/+}$ transgenic mice to *Lama4*$^{-/-}$ and *Tek-cre::Lama5*$^{-/-}$ hosts and their corresponding WT littermates to generate bone marrow chimeras for *in vivo* tracking of monocytes and specifically induced monocyte extravasation by intra-scrotal injection of CCL2 (27). To ensure that extravasating CX3CR1-GFP cells were indeed predominantly myeloid cells and not DCs or NK T cells, cremaster muscles of WT chimeras were stained with anti-Gr-1 which detects both Ly6C$^+$ monocytes and Ly6G$^+$ neutrophils. This confirmed overlap between GFP$^+$ and Gr-1$^+$ cells with the exception of few GFP-negative/Gr-1$^+$ cells that represent neutrophils (**Figure S1A**). Postcapillary venules in the cremaster muscle were intravitally imaged for 2 or 4 h and the extent of monocyte extravasation was determined by quantification of GFP$^+$ cells in an area extending 75 μm from each side of a vessel over a distance of 100 μm vessel length (representing 1.5×10^4 μm^2 tissue area); GFP$^+$ cells adherent to the vessel lumen for 30 sec in a 307 μm length were counted and expressed relative to the surface area of the cylinder vessel tube (**Figure 1A**, **Figures S1B, C**, and **Movie 1**) (8, 28).

The number of adherent GFP$^+$ monocytes in postcapillary venules was similar in the three chimeras (**Figures 1B, C**). However, the number of extravasated GFP$^+$ monocytes at 4 h after CCL2 application was significantly lower in *Lama4*$^{-/-}$ hosts compared to WT hosts (**Figure 1B**). By contrast, significantly higher numbers of GFP$^+$ monocytes had extravasated at 2 h in *Tek-cre::Lama5*$^{-/-}$ hosts compared to WT littermates, but this difference was no longer detectable at 4 h (**Figures 1B, C**), suggesting that monocytes migrated faster across postcapillary venules that lack laminin α5. To more precisely identify extravasated cells, tissues were excised following intravital imaging and examined by confocal microscopy for expression of both GFP and MHCII which is only induced upon extravasation (5); staining for endothelial basement membrane permitted localization of the monocytes within or outside vessels. This revealed a higher proportion of GFP$^+$MHCII$^+$ double positive cells in *Lama4*$^{-/-}$ hosts which, however, remained associated with laminin 511 positive vessels compared to WT controls (**Figures 1D, F**) and *Tek-cre::Lama5*$^{-/-}$ hosts (**Figures 1E, G**). In *Tek-cre::Lama5*$^{-/-}$ hosts most GFP$^+$ cells were located outside of the vessels and showed minimal MHCII expression (**Figures 1E, G**), suggesting that even though more cells extravasated their differentiation toward macrophages was hampered.

Monocyte Accumulation at Laminin α5^{high} Sites

As reported for other leukocytes (7–9), extravasating CX3CR1-GFP$^+$ cells localized preferentially at laminin α5^{low} sites in WT hosts (**Figure 2A**); however, extensive accumulation of CX3CR1-GFP$^+$ cells also occurred within laminin α5^{high} vessels (**Figure 2A**), which was not observed in TNF-α induced neutrophil extravasation (8) probably because of their faster extravasation compared to monocytes and, hence, absence of accumulation within vessel lumens.

As CX3CR1-GFP^{low} monocytes have been reported to mark extravasating inflammatory monocytes (2, 3), we investigated CX3CR1-GFP mean fluorescence intensity (MFI) in relation to laminin α5 high and low regions. CCL-2 induced monocyte extravasation was performed in chimeric mice in which Alexa 650-labeled anti-laminin α5 was injected intra-scrotally to visualize laminin α5 (8) (**Movie 2**) (3). CX3CR1-GFP MFI was measured in areas of high and low laminin 511 expression using dynamic *in situ* cytometry, confirming a higher proportion of CX3CR1-GFP^{low} cells at laminin 511^{low} than at laminin 511^{high} sites, and correspondingly higher proportions of CX3CR1-GFP^{high} monocytes at laminin 511^{high} sites (**Figure 2B** and **Figure S2A**). Correlation of CX3CR1-GFP MFI with speeds of cell migration, revealed that CX3CR1-GFP^{low} monocytes had higher average speeds of migration than CX3CR1-GFP^{high} monocytes (**Figure S2B** and **Figure 2C**), as expected for extravasating cells. In *Lama4*$^{-/-}$ hosts, which show a compensatory ubiquitous expression of laminin 511 in all endothelial basement membranes and the absence of laminin 511 low patches at postcapillary venules (7), all CX3CR1-GFP$^+$ cells showed migration speeds similar to those measured for monocytes at laminin 511^{high} sites in WT hosts, while in *Tek-cre::Lama5*$^{-/-}$ hosts, CX3CR1-GFP$^+$ cells showed higher average migration velocities (**Figure 2D**). Taken together, this suggests that the more motile CX3CR1-GFP^{low} inflammatory monocytes preferentially extravasate at laminin 511^{low} sites.

Mouse Monocyte Adhesion on Laminins *In Vitro*

Monocytic cell lines (U-937, THP-1, Mono Mac 6) have been previously reported to bind to endothelial laminins (29) and macrophages have been reported to bind and migrate on the non-endothelial laminin 111 (11). However, a comprehensive comparison of monocyte and macrophage binding to the endothelial laminins, laminin 411 and 511, and receptor involvement has not been carried out. As it is not possible to obtain sufficient mouse primary CX3CR1-GFP monocytes for *in vitro* adhesion and migration assays, mouse monocyte-like Hoxb8 cells (19) and primary human monocytes were compared to bone marrow derived mouse macrophages (BMDM). Control substrates included ICAM-1 and VCAM-1, which are recognized by αLβ2 (LFA-1) and α4β1, respectively. Human monocytes (**Figure 3A**), mouse Hoxb8 monocytes

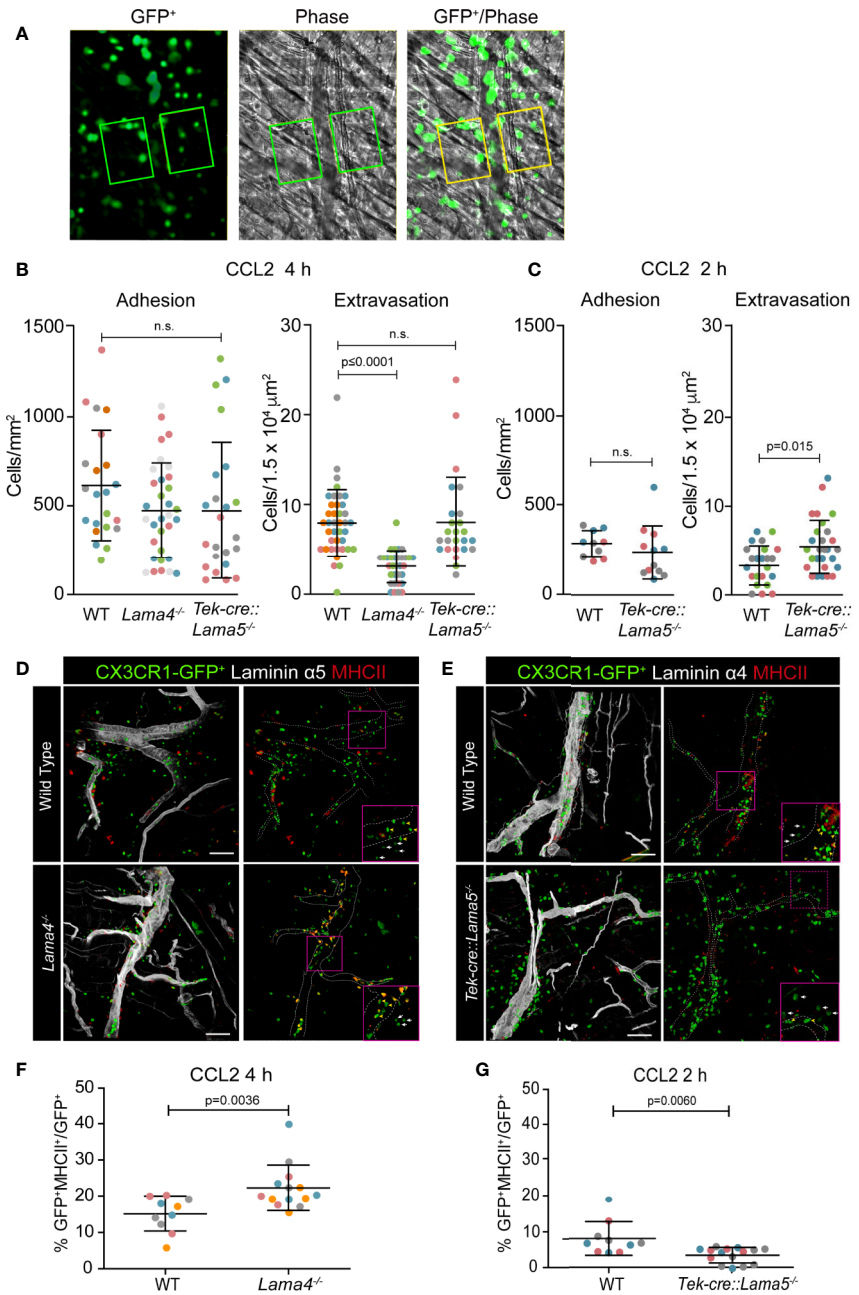

FIGURE 1 | Intravital microscopy of CCL-2 induced monocyte extravasation in cremaster muscle postcapillary venules of *Lama4*$^{-/-}$ or *Tek-cre::Lama5*$^{-/-}$ hosts carrying CX3CR1$^{GFP/+}$ bone marrow. **(A)** Representative fluorescence and corresponding phase contrast images from movies of CX3CR1-GFP^{+} cells extravasating across postcapillary venules of the cremaster muscle; boxed areas, extending from the border to 75 µm either side of postcapillary venules for a length of 100 µm, were used to quantify extravasated CX3CR1-GFP^{+} cells; scale bars = 50 µm; n.s. = non-significant. Quantification of adherent and extravasating CX3CR1-GFP^{+} monocytes at **(B)** 4 h and/or **(C)** 2 h post-application of CCL2. Data are means ± SD from five WT mice and four mice for each chimera with four to eight postcapillary venules examined/mouse at 4 h and three to four WT and chimeric mice with three to four postcapillary venules examined/mouse at 2 h. **(D, E)** Excised tissues were immunofluorescently stained for MHCII and laminin α5 or α4 to identify CX3CR1-GFP^{+}MHCII^{+} extravasating cells in relation to the endothelial basement membrane; dotted lines denote vessel borders; boxed areas are shown in inserts in the lower right hand corners at high magnifications to illustrate patrolling (yellow arrowheads) versus inflammatory monocytes (white arrows); scale bars = 50 µm. **(F, G)** Quantification of proportions of CX3CR1-GFP^{+}MHCII^{+} cells expressed as percentage of total GFP^{+} cells in *Lama4*$^{-/-}$ or *Tek-cre::Lama5*$^{-/-}$ hosts. Data are means ± SD from four WT and four chimeric mice with two to four postcapillary venules examined/mouse in **(F)** and three WT and three chimeric mice with three to seven postcapillary venules examined/mouse in **(G)**. In **(B, C, F, G)** each dot or square denotes one mouse and the different experiments are marked by different colors; significance was calculated using Mann-Whitney tests as not all data passed the normality test by D`Agostino & Pearson; the exact *p*-values are shown in the graphs.

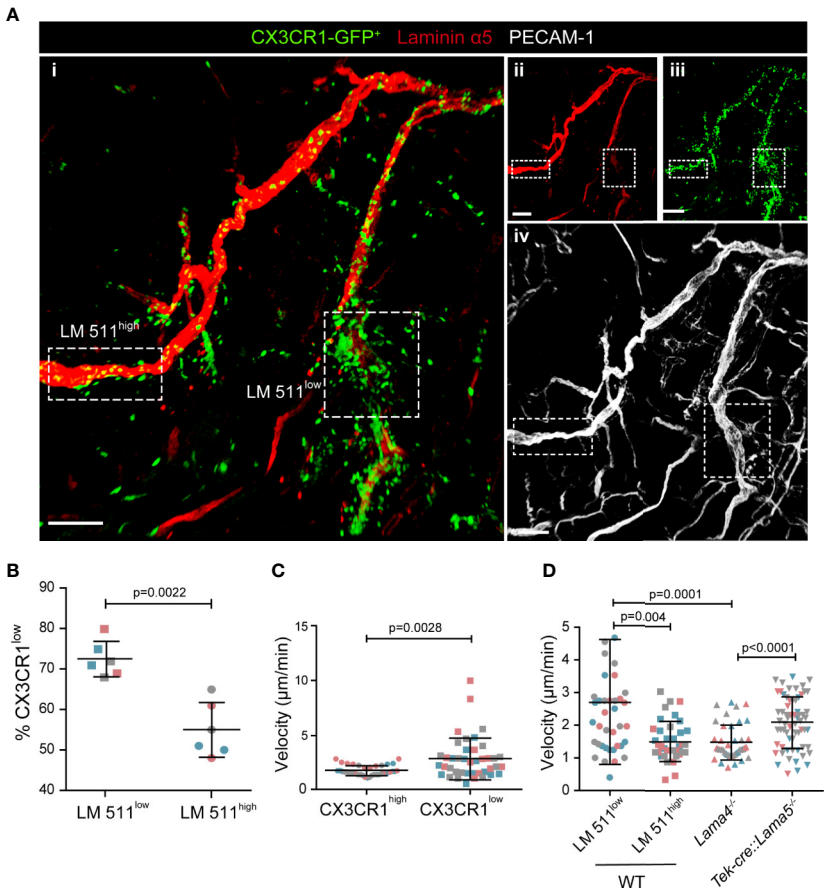

FIGURE 2 | CX3CR1-GFP^{low} inflammatory monocytes preferentially extravasate at laminin 511^{low} sites. **(A)** Representative confocal microscopy of whole mount cremaster muscle from a WT host carrying CX3CR1$^{GFP/+}$ bone marrow stained with anti-laminin α5 and anti-PECAM-1 antibodies (i); single channel images are shown in (ii, iii, iv); scale bar = 100 μm. Experiment was repeated three times with one animal with the same results. **(B)** To track CX3CR1-GFP^{low} inflammatory monocytes GFP mean fluorescence intensity (MFI) was measured *in situ* in areas of high and low laminin 511 expression (see Fig. S2A), revealing a higher proportion of CX3CR1-GFP^{low} cells, expressed as a percent of total GFP^{+} cells, at laminin 511^{low} compared to laminin 511^{high} sites; data are means ± SD of three mice from three separate experiments and at least five postcapillary venules in two different areas/mouse; different experiments are marked by different colors. **(C)** Quantification of GFP MFI and migration speed of individual CX3CR1^{high} and CX3CR1^{low} cells analyzed in three WT hosts from three separate experiments. **(D)** Average migration velocities of extravasating GFP^{+} cells at laminin 511 low and high sites in WT controls, and in *Lama4*$^{-/-}$ and *Tek-cre::Lama5*$^{-/-}$ chimeras. Data in **(C, D)** are means ± SD calculated from 39-64 cells analyzed in three mice per chimera (marked by different colors); movies were captured at 4 h post-administration of CCL2. Significance of data in **(B–D)** were calculated using Mann-Whitney tests since the data did not pass the normality test by D`Agostino & Pearson; the exact *p*-values are shown in the graph.

(**Figure 3B**) and mouse BMDM (**Figure 3C**) showed extensive binding to laminin 511 and VCAM-1, and lower binding to laminin 411 (**Figures 3A, B**). However, human monocytes and mouse Hoxb8 monocytes also showed high levels of binding to BSA and ICAM-1, probably due to activation of integrin β2, which we have previously shown indiscriminately enhances non-specific binding of neutrophils to all substrates including BSA and plastic (6) (**Figures 3A, B**). Therefore, mouse integrin β2 null (CD18$^{-/-}$) (20) Hoxb8 monocytes were generated and employed in all subsequent adhesion assays, and human monocytes were treated with anti-human integrin β2 blocking antibody (TS1/18). This significantly reduced binding to ICAM-1 and BSA, and revealed specific binding to laminin 511 and VCAM-1 for all cells (**Figures 3A–C**); only mouse BMDM also showed binding to laminin 411 (**Figure 3C**).

Flow cytometry revealed similar expression patterns for the main laminin binding integrins on WT and CD18$^{-/-}$ mouse Hoxb8 and human monocytes and BMDM which suggested expression of integrins α6β1, α5β1 and αvβ1, and/or αvβ3 (**Figure S3**), with higher levels of α6β1, αvβ1, and αvβ3 and the unique expression of integrin α3β1 on BMDM (30–32). To test integrin involvement in binding to the laminins, function blocking antibodies to integrins α6, β1, or β3 were employed in adhesion assays, revealing complete inhibition of mouse Hoxb8 and human monocytes binding to laminin 511 by anti-integrin β1 and α6 antibodies (**Figures 3D, E**). In the case of BMDM, anti-integrin β1 and α6 antibodies also ablated binding to laminin 411 but only partially inhibited binding to laminin 511, suggesting the involvement of other receptors (**Figure 3F**). Partial inhibition by anti-integrin β3 suggests the involvement of

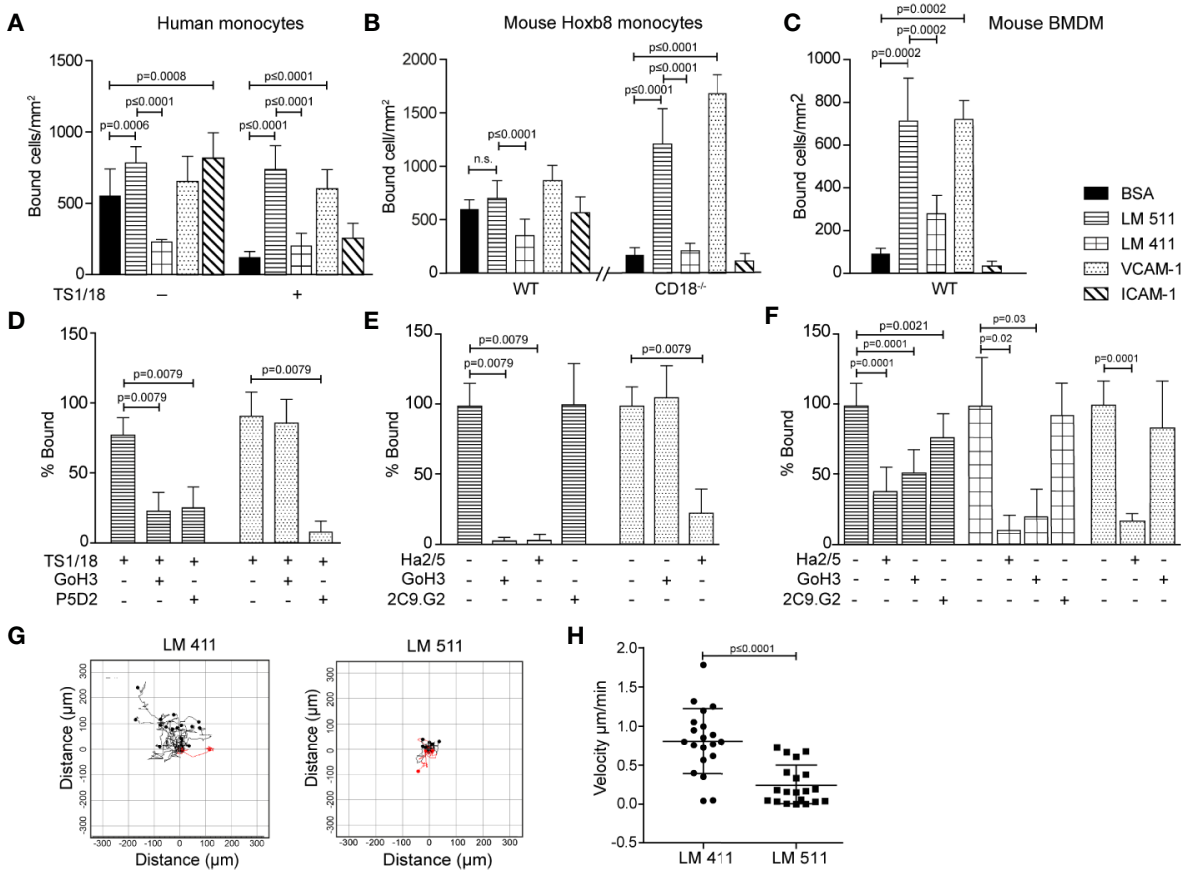

FIGURE 3 | Human monocytes, mouse monocyte-like Hoxb8 cells and mouse bone marrow derived macrophages (BMDM) bind differentially to endothelial laminins. Human monocytes **(A, D)**, mouse monocyte-like Hoxb8 cells **(B, E)** and BMDM **(C, F)** adhesion to laminins 411, 511, VCAM-1, ICAM-1, or BSA. To exclude non-specific integrin β2-mediated adhesion of monocytic cells, experiments were performed with untreated or integrin β2 antibody (TS1/18) treated human monocytes, and WT and CD18$^{-/-}$ mouse monocyte-like Hoxb8 cells. Adherent cells were counted at 1 h and expressed as number of bound cells/mm^2. **(D)** Inhibition assays were performed with human monocytes preincubated with TS1/18 and either anti-integrin α6 (GoH3) or β1 (P5D2) antibodies before addition to substrates. Similar experiments were performed with mouse monocyte-like CD18$^{-/-}$ Hoxb8 cells **(E)** and BMDM **(F)** pre-incubated with anti-mouse integrin β1 (Ha2/5), α6 (GoH3), or β3 (2C9.G2) antibodies. Data in **(D–F)** are expressed as percent of total cells bound in the absence of blocking antibodies. All data except **(F)** are means ± SD from four to five independent experiments with triplicates/experiment; **(F)** are means ± SEM of three experiments with triplicates/experiment. **(G)** Random migration of BMDM on laminin 411 and laminin 511 were imaged by time-lapse video microscopy; >20 cells on each substrate were tracked and analyzed, and **(H)** velocity of migrating cells on each substrate; data are means ± SD from a representative experiment. The experiment was performed three times with similar results. Significance was calculated using a Mann-Whitney test in **(A, C, D, E, H)**, a Welch's t-test in **(B)**, and an unpaired t-test in **(F)**; exact *p*-values are shown in the graph; n. s.= non-significant.

αvβ3 (**Figure 3F**), although αvβ1 cannot be excluded. While integrin α3β1 can also bind to laminin 511 (30–32), the absence of function blocking antibodies against the mouse protein prevented investigation of whether this is the case in BMDM. This suggests that α6β1 is the major laminin 511 receptor on mouse and human monocytes (31) while BMDMs also employ an αv series integrin, and potentially also α3β1, to bind laminin 511 and, additionally, bind to laminin 411 *via* integrin α6β1.

Migration Assays

We have previously shown that monocytes migrate equally well across laminin 411, 511 or non-endothelial laminin 111 in a transwell assay (7). This pattern was not altered by plating endothelial cells onto the laminin substrates (**Figures S4A, B**), as we have shown occurs with other immune cell types (8), nor did the mouse HoxB8 monocytes, human monocytes or mouse BMDM employed here express laminin proteins (**Figure S5**) which has been proposed by others to affect the extravasation process (29). However, BMDM migration on laminin 411 and 511 did differ: As macrophages are unlikely to transmigrate across endothelial monolayers and their basement membranes *in vivo*, we analyzed 2D chemotaxis of BMDM using time-lapse video microscopy, revealing BMDM migration on both laminins 411 and 511 but more extensive and faster migration on laminin 411 compared to laminin 511 (**Figures 3G, H**). Hence, even though macrophages in general migrate more slowly than other leukocytes (33), they can distinguish between laminins 411 and 511 and migrate differently on these substrates.

Monocyte *In Vivo* Differentiation

As monocytes and macrophages have different migration capacities on different substrates (11, 12, 34) and monocytes have been reported to initiate gene expression changes toward a more differentiated MHCII$^+$ phenotype upon extravasation (5, 35), we investigated the possibility of *in vivo* modulation of the monocyte phenotype during extravasation process.

As it is not possible to isolate sufficient leukocytes from the cremaster muscle to phenotype the extravasated GFP$^+$ cells, we investigated the intestine where resident macrophages of the lamina propria (LP) are constantly replenished by circulating monocytes (36) and extravasate across postcapillary venules. Differentiating monocytes and macrophages, therefore, represent a large fraction of the total LP cells and are well characterized by their differential expression of cell surface markers (**Figure S6A**). This permits categorization into early extravasated Ly6C^{high}MHCII^{low} immature P1 and maturing Ly6C^{high}MHCII^{high} P2 populations, and mature Ly6C^{low}MHCII^{high} P3 macrophages (22).

Postcapillary venules of the colon wall showed the same patchy laminin α5 and even laminin α4 distribution as occurs in other tissues (**Figure S6B**). LP cells from colons of *Lama4*$^{-/-}$ and *Tek-cre::Lama5*$^{-/-}$ mice and WT controls were analyzed by flow cytometry using the gating strategy outlined in **Figure S6A** at adult stages (3 months old) (**Figures 4A–C**) and at post-natal day 21 (P21) (**Figures 4D, E** and **Figure S6C**). The latter stage represents the peak of colonization of intestinal macrophages by circulating monocytes. In P21 samples, P1 and P2 early extravasating populations were analyzed together due to the lower numbers of cells obtained (**Figure S6C**). In both adult and P21 LP, fewer early extravasating P1 and P2 cells were measured in *Lama4*$^{-/-}$ and more in *Tek-cre::Lama5*$^{-/-}$ compared to WT mice (**Figures 4B, D**), reflecting the same pattern of results that were observed in the intravital imaging studies in the cremaster muscle (**Figures 1A, B**). However, despite fewer extravasating monocytes, a larger P3 mature macrophage population was measured in *Lama4*$^{-/-}$ LP than in either WT or *Tek-cre::Lama5*$^{-/-}$ LP as reflected by higher P3/P2 ratios (**Figures 4C, E**). By contrast, *Tek-cre::Lama5*$^{-/-}$ LP showed lower proportions of P3/P2 ratios than *Lama4*$^{-/-}$ and WT LP (**Figures 4C, E**), which was particularly evident in P21 LP (**Figure 4E** and **Figure S6C**) where a larger proportion of macrophages are derived from infiltrating monocytes (22). These results suggest that in the absence of endothelial basement membrane laminin 511, monocyte differentiation to macrophages is reduced and promoted when only laminin 511 is present as occurs in the *Lama4*$^{-/-}$ and WT LP. Flow cytometry analyses of the main laminin binding integrins, α6 and αv, on P1, P2, and P3 populations in adult and P21 LP, revealed higher levels of integrin αv in P3 macrophages (**Figure 4F**) as also observed in BMDM (**Figure S3C**); however, integrin α3 was not detectable on P1, P2 or P3 populations from adult or P21 tissues.

Mouse Splenic Derived Monocyte Differentiation *In Vitro*

Splenic monocyte interaction with vascular endothelium has been previously shown to promote differentiation to macrophages in an *in vitro* model (5); we therefore tested the role of laminin 511 in the same experimental setup. Endothelioma cell lines were generated from *Lama4*$^{-/-}$ and WT littermate embryos (18) which expressed high (eEND4.1) or low (eENDwt) levels of laminin α5, respectively (**Figure S7A**). However, despite several attempts it was not possible to establish an endothelioma cell line from *Tek-cre::Lama5*$^{-/-}$ embryos as the cells did not proliferate; similar results were obtained using CRISPR/Cas 9 to eliminate *Lama5* expression in the bEND.5 cell line (manuscript in preparation). Naïve splenic monocytic cells (**Figure S7B**) were incubated on confluent monolayers of eENDwt or eEND4.1 for 16 h and cells localised at the subendothelial layer were analyzed by flow cytometry as described previously (5), revealing a significantly higher proportion of MHCII$^+$Ly6C^{neg} and F4/80$^+$Ly6C^{neg} macrophages in eEND4.1 than in eENDwt cocultures (**Figures 5A, B**). When the same experiments were performed with splenocytes preincubated in the presence of a function blocking antibody to integrin α6β1, the proportions of MHCII$^+$Ly6C^{neg} and F4/80$^+$Ly6C^{neg} macrophages in the eEND4.1 cultures were reduced to levels observed in eENDwt cultures (**Figures 5A, B**). This substantiates a role for endothelial cell-derived laminin 511 in promoting monocyte differentiation to macrophages, and suggests the involvement of both the endothelium and a direct integrin α6β1-mediated interaction with laminin 511.

As laminins may affect the expression of cytokines by endothelium which in turn may affect monocyte differentiation, we measured cytokine profiles in the conditioned medium of eEND4.1 and eENDwt cells cultured alone or co-cultured with the splenic monocytes, and of splenic monocytes alone under the same conditions as described above. Cytokines examined are those implicated in monocyte to macrophage differentiation, including GM-CSF, IL-6, IL-10, IFN-γ, TNF-α, and IL-1α (37). Significant levels of cytokines were measured only in cocultures of eENDwt or eEND4.1 together with splenic monocytes, with lower levels of IL-6, IL-10, and IFN-γ in cocultures with eEND4.1 cells compared to eENDwt cells, but no changes in GM-CSF, TNF-α, and IL-1α (**Figure 5C**). Although monocytes and macrophages are the main sources of these cytokines, some such as GM-CSF, IL-6, IL-1, and IL-10 can also be secreted by endothelial cells. The fact that there was no substantial secretion of these cytokines from eEND4.1 cells cultured alone suggests that laminin 511 does not affect endothelial expression of cytokines but rather that the cytokines stem from the differentiating monocytes. These data also further substantiate the hypothesis that monocyte interaction with both the endothelium and with laminin 511 are required for efficient triggering of macrophage differentiation. The pattern of cytokines observed in the eEND4.1/splenic monocyte cocultures suggests that laminin 511 promotes a non-inflammatory macrophage population (37).

DISCUSSION

`Published data suggest that monocyte interaction with the endothelium during extravasation is a critical step in the switch to macrophage differentiation (5). Our data demonstrate that it is

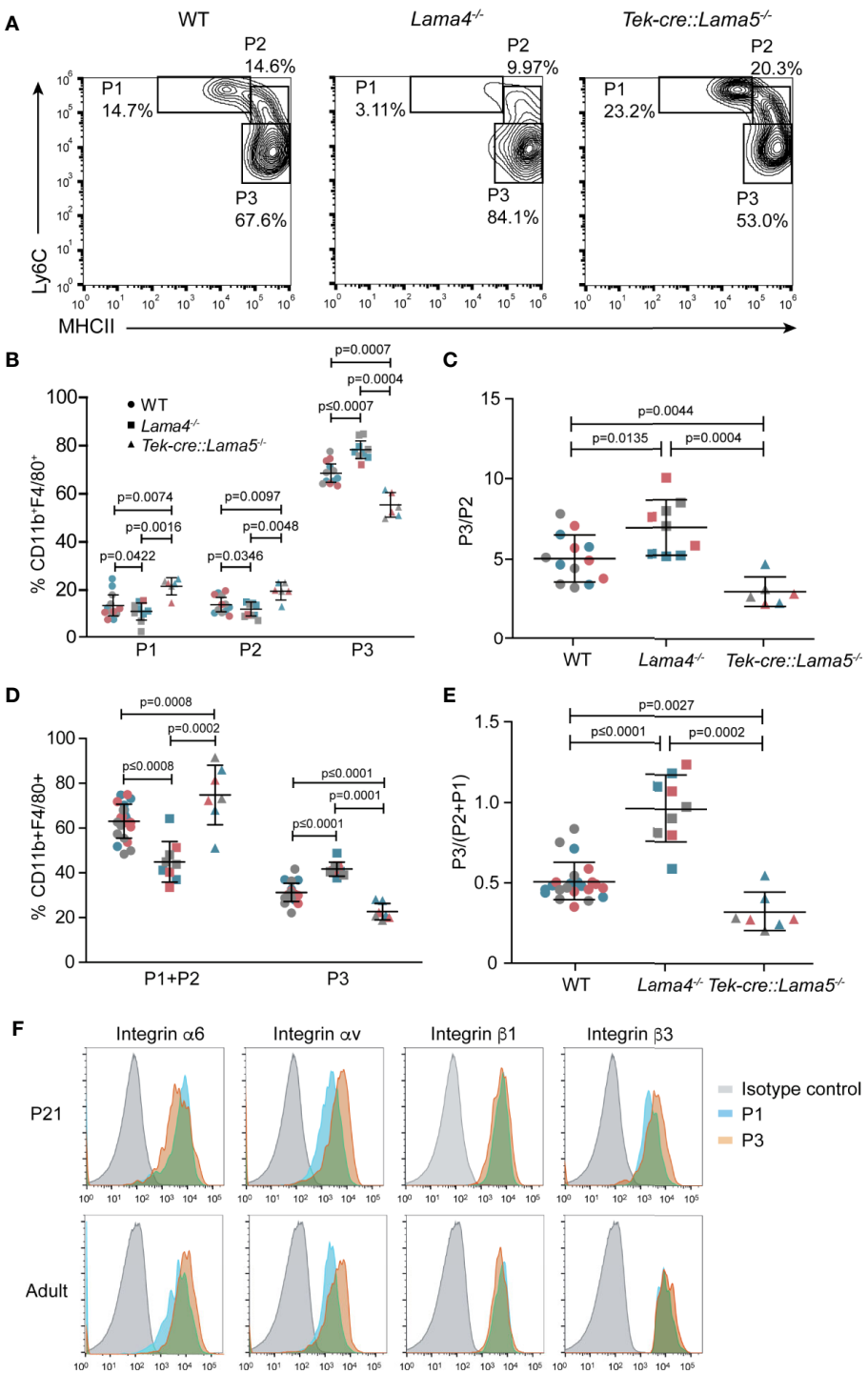

FIGURE 4 | Monocyte differentiation in colons of *Lama4*$^{-/-}$ and *Tek-cre::Lama5*$^{-/-}$ mice. **(A)** Representative flow cytometry showing proportions of early extravasating P1 (Ly6C^{hi}MHCII^{low}) and P2 (Ly6C^{mid}MHCII^{mid}) populations, and mature P3 macrophages (Ly6C^{low}MHCII^{hi}) in isolated colonic lamina propria cells from adult WT, *Lama4*$^{-/-}$ and *Tek-cre::Lama5*$^{-/-}$ mice; **(B)** corresponding quantification of the data and **(C)** ratios of P3/P2 cells. Data are means ± SD from three independent experiments (marked in different colors) performed with 13 WT, 9 *Lama4*$^{-/-}$, and 6 *Tek-cre::Lama5*$^{-/-}$ mice. **(D)** Corresponding analyses of P1 plus P2 populations, and mature P3 macrophages amongst colonic lamina propria cells of P21 WT, *Lama4*$^{-/-}$ and *Tek-cre::Lama5*$^{-/-}$ mice; and **(E)** ratios of P3/P2+P1 cells. Data are means ± SEM from three experiments (marked in different colors) performed with 23 WT, 9 *Lama4*$^{-/-}$, and 7 *Tek-cre::Lama5*$^{-/-}$ mice (marked by different symbols). Significance of the data was calculated using a Mann-Whitney test; exact *p*-values are shown in the graph. **(F)** Representative flow cytometry of laminin binding integrins on colon P1, P2, and P3 cells from adult and P21 WT mice. The experiment was repeat three times with the same pattern of results.

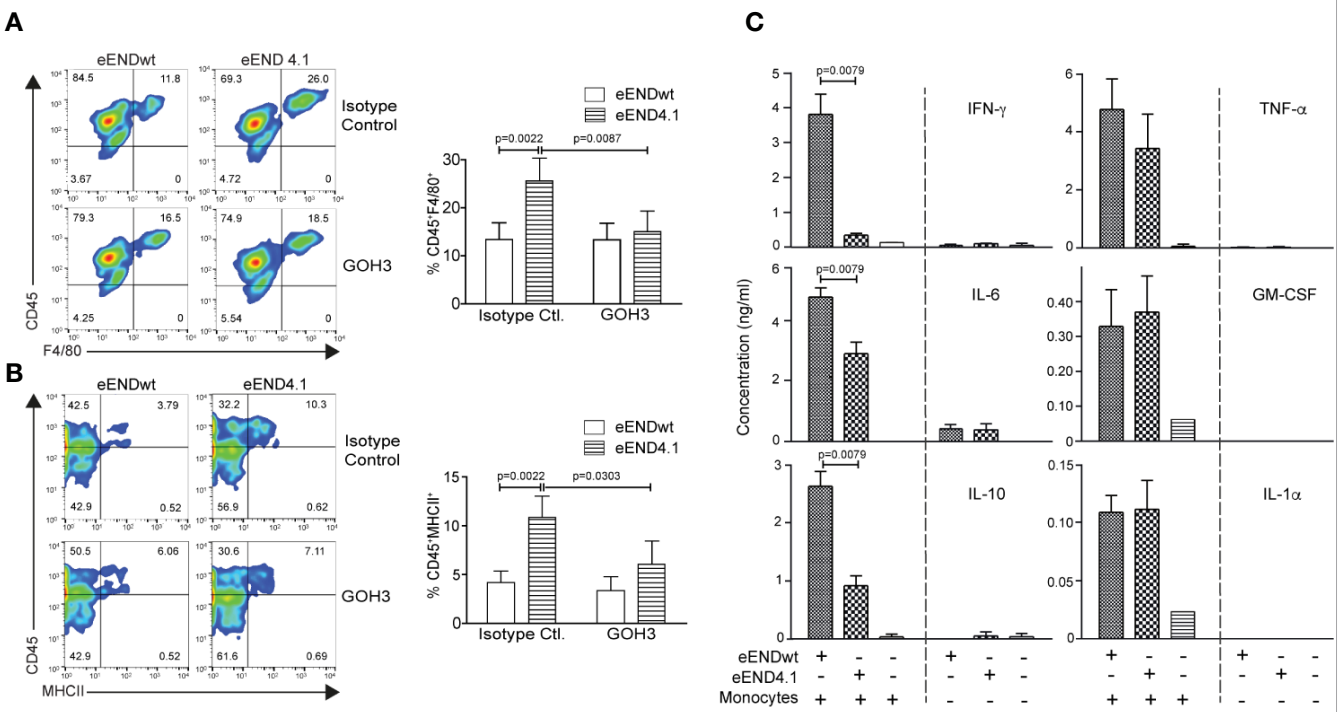

FIGURE 5 | Enhanced *in vitro* differentiation of splenic monocytes to macrophages on laminin 511-overexpressing endothelial cells. Representative flow cytometry for **(A)** $CD45^+F4/80^+$ and **(B)** $CD45^+MHCII^+$ in splenic monocytes cocultured for 16 h with eENDwt or eEND4.1 cells in the presence or absence of integrin α6 blocking (GoH3) antibody; bar graphs show quantification of the data expressed as a percent of the total $CD45^+$ population. Isotype control antibody had no effect. Data are means ± SD from three experiments with two replicates/experiment/treatment. Significance was calculated using a Mann-Whitney test; exact *p*-values are shown in the graph. **(C)** Cytokine concentrations in conditioned media of eENDwt or eEND4.1 cells cultured in the presence or absence of splenic monocytes for 16 h, and of splenic monocytes alone. Data are means ± SD of 3 experiments performed with duplicates/experiment. Absence of values indicates that the cytokines were not detectable. Significance was calculated using a Mann-Whitney test; exact *p*-values are shown in the graph.

not the endothelium alone but also laminin 511 in the underlying basement membrane that is required for this switch.

Like T cells and neutrophils, $CX3CR1\text{-}GFP^+$ monocytes also preferentially extravasated at laminin 511^{low} sites, with $CX3CR1\text{-}GFP^{low}$ inflammatory-monocytes showing preferential localization and higher motility at such sites. However, *in vitro* transmigration studies revealed an equal ability of monocytes to migrate across both endothelial laminins and non-endothelial laminins and BSA. While this may reflect shortcomings of the *in vitro* experimental systems employed, we propose that high affinity binding of the infiltrating monocytes to laminin 511 in the endothelial basement membrane traps them at this site and promotes their differentiation toward the macrophage lineage, which alters both their integrin profile and migratory mode. Both monocytes and macrophages bind efficiently to laminin 511 but only macrophages bind to laminin 411 and can, therefore, distinguish between these two isoforms; they also migrate more efficiently on laminin 411, explaining the faster extravasation of $CX3CR1\text{-}GFP^+$ cells in *Tek-cre::Lama5*$^{-/-}$ hosts. This highlights the site between the endothelial monolayer and the underlying basement membrane as a critical site for the modulation of the phenotype of infiltrating monocytes and for their switch to macrophages. This is supported by the enhanced macrophage differentiation of splenic monocytes observed in cocultures with laminin 511 overexpressing endothelial cell lines and also the data obtained from the intestines of the laminin knockout mice.

Macrophage colonization of the intestine at P21 and their replenishment in adult animals requires monocyte extravasation across the endothelial monolayer of postcapillary venules and the underlying basement membrane in order to enter into the stroma between the intestinal crypts; as in inflammation, this step is dependent on CCL2 (38). The process, therefore, is similar to monocyte extravasation during inflammation and provides a unique model for investigating monocyte differentiation to macrophages. While several factors such as colony stimulation factor 1 (CSF1) and TGF-β have been shown to play important roles in this switch in the intestine, current data suggests that additional factors must be involved (36, 39). Since laminin 411 and 511 are localized in the endothelial basement membrane, the higher proportion of differentiated P3 macrophages in the intestine LP of both P21 and mature *Lama4*$^{-/-}$ mice and lower proportions in *Tek-cre::Lama5*$^{-/-}$ mice suggest that the switch to macrophages is induced at the level of the endothelial basement membrane,

i.e., before the macrophages enter the intestinal stroma, and furthermore is promoted by laminin 511. This is consistent with reports that adhesion of monocytes to endothelium triggers expression of extravasation specific genes initiating changes toward a more differentiated phenotype (35, 40) and that specifically the site underlying endothelial cells, but not fibroblasts, is critical for this switch (5). Taken together with our data this suggests that laminin 511 plus the endothelium provide an early signal that promotes the switch of monocytes to macrophages. The fact that blocking integrin α6 reduced, but did not ablate, the differentiation of monocytes incubated with endothelium overexpressing laminin 511 to macrophages suggests that two steps are involved—cross-talk with the endothelium, in an as yet undefined manner, and integrin α6β1 mediated interaction with laminin 511 in the endothelial basement membrane. The absence of such an effect in monocytes incubated with fibroblasts (5) may be explained by the nature of extracellular matrix that fibroblasts secrete, which is mainly collagen types I and III and proteoglycans and, in specialized situations, also laminins 411 and 211 (41–43) but not laminin 511 (44). The relatively long incubation time of monocytes with endothelium required for the *in vitro* differentiation to macrophages (16 h), compared to the time required for monocytes to extravasate into the inflamed cremaster muscle (2–4 h), suggests the absence of critical factors in the *in vitro* setup, which may include absence of a mature basement membrane that cannot be recapitulated *in vitro* using cultured cells.

There is increasing evidence that molecularly distinct steps exist subsequent to penetration of the endothelial monolayer that are critical for successful extravasation into inflamed tissues. This is suggested by intravital microscopy studies (8, 45) and by studies involving blocking of endothelial junctional molecules, such as CD99, CD99L and PECAM-1, that result in leukocyte arrest at cell-cell junctions or at the endothelial basement membrane (8, 46–49). However, the concept that endothelial barrier function and phenotypes of extravasating immune cells may be affected by signals originating from the endothelial basement membrane, as suggested here, is only starting to emerge. How basement membrane components affect extravasation is likely to depend on the immune cell and tissue type, e.g., the effects on highly impermeable microvessels of the central nervous system are likely to differ from those on the microvessels of secondary lymphoid organs. Recent data from our lab supports a role for endothelial laminins 511 and 411 in modulating the pathogenicity of T cells infiltrating into the brain during neuroinflammation (10). While the integrins and mechanisms involved are different to those described here, the data reinforce the sub-endothelial site as important for modulation of immune cell phenotypes during extravasation processes.

We show here that the switch toward a macrophage phenotype is associated with a change in integrin profile, as reported previously by others (12, 50, 51), with the notable unique expression of integrin α3β1 by BMDM and increased surface levels of αvβ1/αvβ3 and α6β1, all of which can bind to laminin 511 and, in the case of α6β1 and α3β1, also laminin 411 (30, 52). Such changes are likely to affect the ability of the cells to interact with and to distinguish between the different laminin isoforms. However, differentiation toward the macrophage lineage is also associated with changes in size and cytoplasmic complexity (53) that will affect migration potential and speed. The larger size of macrophages (15–20 μm) compared to monocytes (7–8 μm) may contribute to their slower migration (33, 54), but the associated larger cytoplasmic volume and more complex cytoskeleton may be an advantage with respect to the force required to penetrate the endothelial basement membrane *in vivo*—topics that require future investigation. Indeed, it may be serendipitous whether an extravasating monocyte encounters a laminin 511 high or low patch in the postcapillary venule basement membrane, which may determine those cells that differentiate toward the macrophage phenotype and those that do not and can re-enter the circulation (53), placing endothelial laminin 511 in a pivotal position in the switch from monocytes to macrophages. While we have here specifically examined monocytes/macrophages, the processes and concepts described may be relevant to other differentiation processes involving cells located at such vascular niches, including stem cells.

DATA AVAILABILITY STATEMENT

The raw data supporting the conclusions of this article will be made available by the authors, without undue reservation.

ETHICS STATEMENT

The animal study was reviewed and approved by Landesamt für Natur, Umwelt und Verbraucherschutz, Nordrhein-Westfalen; Aktenzeichen 81-02.04.2018.A392.

AUTHOR CONTRIBUTIONS

LL carried out the intravital microscopy (IVM) experiments and most adhesion and migration assays. JS analyzed all IVM experiments and carried out all *in vitro* macrophage differentiation experiments. SL performed adhesion assays with WT and $CD18^{-/-}$ Hoxb8 monocytes; OC performed flow cytometry of Hoxb8 monocytes and BMDM. TV generated WT and $CD18^{-/-}$ Hoxb8 monocyte lines and contributed to writing of the manuscript. JR contributed to experimental design and writing of the manuscript. RH generated and characterized endothelioma cell lines and, together with M-JH, contributed to experimental design, analyses of data, and writing of the manuscript. LS designed the project, supervised all work, and wrote the original manuscript. All authors contributed to the article and approved the submitted version.

FUNDING

This work was supported by funding from the German Research Foundation (CRC1009A02, B08, B09, and EXE1003).

ACKNOWLEDGMENTS

We thank Sigmund Budny for purification of laminins, Barbara Liel for generation of eENDwt and eEND4.1 cells, and Hanna Gerwien for all statistical analyses. This manuscript has been released as a pre-print at BioRxiv https://www.biorxiv.org/content/10.1101/2020.04.15.043190v1.

SUPPLEMENTARY MATERIAL

The Supplementary Material for this article can be found online at: https://www.frontiersin.org/articles/10.3389/fimmu.2020.584229/full#supplementary-material

REFERENCES

1. Wynn TA, Chawla A, Pollard JW. Macrophage biology in development, homeostasis and disease. *Nature* (2013) 496(7446):445–55. doi: 10.1038/nature12034
2. Auffray C, Fogg D, Garfa M, Elain G, Join-Lambert O, Kayal S, et al. Monitoring of blood vessels and tissues by a population of monocytes with patrolling behavior. *Science* (2007) 317(5838):666–70. doi: 10.1126/science.1142883
3. Gordon S, Taylor PR. Monocyte and macrophage heterogeneity. *Nat Rev Immunol* (2005) 5(12):953–64. doi: 10.1038/nri1733
4. Dal-Secco D, Wang J, Zeng Z, Kolaczkowska E, Wong CH, Petri B, et al. A dynamic spectrum of monocytes arising from the in situ reprogramming of CCR2+ monocytes at a site of sterile injury. *J Exp Med* (2015) 212(4):447–56. doi: 10.1084/jem.20141539
5. Jakubzick C, Gautier EL, Gibbings SL, Sojka DK, Schlitzer A, Johnson TE, et al. Minimal differentiation of classical monocytes as they survey steady-state tissues and transport antigen to lymph nodes. *Immunity* (2013) 39(3):599–610. doi: 10.1016/j.immuni.2013.08.007
6. Sixt M, Engelhardt B, Pausch F, Hallmann R, Wendler O, Sorokin LM. Endothelial cell laminin isoforms, laminin 8 and 10, play decisive roles in in T-cell recruitment across the blood-brain-barrier in an experimental autoimmune encephalitis model (EAE). *J Cell Biol* (2001) 153:933–45. doi: 10.1083/jcb.153.5.933
7. Wu C, Ivars F, Anderson P, Hallmann R, Vestweber D, Nilsson P, et al. Endothelial basement membrane laminin alpha5 selectively inhibits T lymphocyte extravasation into the brain. *Nat Med* (2009) 15(5):519–27. doi: 10.1038/nm.1957
8. Song J, Zhang X, Buscher K, Wang Y, Wang H, Di Russo J, et al. Endothelial basement membrane laminin 511 contributes to endothelial junctional tightness and thereby inhibits leukocyte transmigration. *Cell Rep* (2017) 18(5):1256–69. doi: 10.1016/j.celrep.2016.12.092
9. Wang S, Voisin MB, Larbi KY, Dangerfield J, Scheiermann C, Tran M, et al. Venular basement membranes contain specific matrix protein low expression regions that act as exit points for emigrating neutrophils. *J Exp Med* (2006) 203(6):1519–32. doi: 10.1084/jem.20051210
10. Zhang X, Wang Y, Song J, Gerwien H, Chuquisana O, Chashchina A, et al. The endothelial basement membrane acts as a checkpoint for entry of pathogenic T cells into the brain. *J Exp Med* (2020) 217(7):e20191339. doi: 10.1084/jem.20191339
11. Mercurio AM, Shaw LM. Macrophage interactions with laminin: PMA selectively induces the adherence and spreading of mouse macrophages on a laminin substratum. *J Cell Biol* (1988) 107(5):1873–80. doi: 10.1083/jcb.107.5.1873
12. Shaw LM, Lotz MM, Mercurio AM. Inside-out integrin signaling in macrophages. Analysis of the role of the alpha 6A beta 1 and alpha 6B beta 1 integrin variants in laminin adhesion by cDNA expression in an alpha 6 integrin-deficient macrophage cell line. *J Biol Chem* (1993) 268(15):11401–8.
13. Cougoule C, Van Goethem E, Le Cabec V, Lafouresse F, Dupre L, Mehraj V, et al. Blood leukocytes and macrophages of various phenotypes have distinct abilities to form podosomes and to migrate in 3D environments. *Eur J Cell Biol* (2012) 91(11-12):938–49. doi: 10.1016/j.ejcb.2012.07.002
14. Thyboll J, Kortesmaa J, Cao R, Soininen R, Wang L, Iivanainen A, et al. Deletion of the laminin alpha4 chain leads to impaired microvessel maturation. *Mol Cell Biol* (2002) 22(4):1194–202. doi: 10.1128/MCB.22.4.1194-1202.2002
15. Song J, Lokmic Z, Lammermann T, Rolf J, Wu C, Zhang X, et al. Extracellular matrix of secondary lymphoid organs impacts on B-cell fate and survival. *Proc Natl Acad Sci USA* (2013) 110(31):E2915–24. doi: 10.1073/pnas.1218131110
16. Di Russo J, Luik AL, Yousif L, Budny S, Oberleithner H, Hofschroer V, et al. Endothelial basement membrane laminin 511 is essential for shear stress response. *EMBO J* (2017) 36(2):183–201. doi: 10.15252/embj.201694756
17. Jung S, Aliberti J, Graemmel P, Sunshine MJ, Kreutzberg GW, Sher A, et al. Analysis of fractalkine receptor CX(3)CR1 function by targeted deletion and green fluorescent protein reporter gene insertion. *Mol Cell Biol* (2000) 20(11):4106–14. doi: 10.1128/MCB.20.11.4106-4114.2000
18. Williams RL, Risau W, Zerwer H-G, Drexler H, Aguzzi A, Wagner EF. Endothelioma cells expressing the polyoma middle T oncogene induce hemangiomas by host cell recruitment. *Cell* (1989) 57:1053–63. doi: 10.1016/0092-8674(89)90343-7
19. Wang GG, Calvo KR, Pasillas MP, Sykes DB, Hacker H, Kamps MP. Quantitative production of macrophages or neutrophils ex vivo using conditional Hoxb8. *Nat Methods* (2006) 3(4):287–93. doi: 10.1038/nmeth865
20. Scharffetter-Kochanek K, Lu H, Norman K, van Nood N, Munoz F, Grabbe S, et al. Spontaneous skin ulceration and defective T cell function in CD18 null mice. *J Exp Med* (1998) 188(1):119–31. doi: 10.1084/jem.188.1.119
21. Lipowsky HH, Zweifach BW. Application of the "two-slit" photometric technique to the measurement of microvascular volumetric flow rates. *Microvasc Res* (1978) 15(1):93–101. doi: 10.1016/0026-2862(78)90009-2
22. Bain CC, Bravo-Blas A, Scott CL, Perdiguero EG, Geissmann F, Henri S, et al. Constant replenishment from circulating monocytes maintains the macrophage pool in the intestine of adult mice. *Nat Immunol* (2014) 15(10):929–37. doi: 10.1038/ni.2967
23. Lenter M, Uhlig H, Hamann A, Jeno P, Imhof B, Vestweber D. A monoclonal antibody against an activation epitope on mouse integrin chain beta 1 blocks adhesion of lymphocytes to the endothelial integrin alpha 6 beta 1. *Proc Natl Acad Sci USA* (1993) 90:9051–5. doi: 10.1073/pnas.90.19.9051
24. Wayner EA, Carter WG, Piotrowicz RS, Kunicki TJ. The function of multiple extracellular matrix receptors in mediating cell adhesion to extracellular matrix: preparation of monoclonal antibodies to the fibronectin receptor that specifically inhibit cell adhesion to fibronectin and react with platelet glycoproteins Ic-IIa. *J Cell Biol* (1988) 107(5):1881–91. doi: 10.1083/jcb.107.5.1881
25. Geissmann F, Jung S, Littman DR. Blood monocytes consist of two principal subsets with distinct migratory properties. *Immunity* (2003) 19(1):71–82. doi: 10.1016/S1074-7613(03)00174-2
26. Bradfield PF, Scheiermann C, Nourshargh S, Ody C, Luscinskas FW, Rainger GE, et al. JAM-C regulates unidirectional monocyte transendothelial migration in inflammation. *Blood* (2007) 110(7):2545–55. doi: 10.1182/blood-2007-03-078733
27. Sallusto F, Baggiolini M. Chemokines and leukocyte traffic. *Nat Immunol* (2008) 9(9):949–52. doi: 10.1038/ni.f.214
28. Voisin MB, Woodfin A, Nourshargh S. Monocytes and neutrophils exhibit both distinct and common mechanisms in penetrating the vascular basement membrane in vivo. *Arterioscler Thromb Vasc Biol* (2009) 29(8):1193–9. doi: 10.1161/ATVBAHA.109.187450

29. Pedraza C, Geberhiwot T, Ingerpuu S, Assefa D, Wondimu Z, Kortesmaa J, et al. Monocytic cells synthesize, adhere to, and migrate on laminin 8. *J Immunol* (2000) 165:5831–8. doi: 10.4049/jimmunol.165.10.5831
30. Kikkawa Y, Sanzen N, Fujiwara H, Sonnenberg A, Sekiguchi K. Integrin binding specificity of laminin-10/11: laminin-10/11 are recognized by alpha 3 beta 1, alpha 6 beta 1 and alpha 6 beta 4 integrins. *J Cell Sci* (2000) 113(5):869–76.
31. Sasaki T, Timpl R. Domain IVa of laminin alpha5 chain is cell-adhesive and binds beta1 and alphaVbeta3 integrins through Arg-Gly-Asp. *FEBS Lett* (2001) 509(2):181–5. doi: 10.1016/S0014-5793(01)03167-2
32. Nishiuchi R, Takagi J, Hayashi M, Ido H, Yagi Y, Sanzen N, et al. Ligand-binding specificities of laminin-binding integrins: a comprehensive survey of laminin-integrin interactions using recombinant alpha3beta1, alpha6beta1, alpha7beta1 and alpha6beta4 integrins. *Matrix Biol* (2006) 25(3):189–97. doi: 10.1016/j.matbio.2005.12.001
33. Bzymek R, Horsthemke M, Isfort K, Mohr S, Tjaden K, Muller-Tidow C, et al. Real-time two- and three-dimensional imaging of monocyte motility and navigation on planar surfaces and in collagen matrices: roles of Rho. *Sci Rep* (2016) 6:25016. doi: 10.1038/srep25016
34. Shaw LM, Mercurio AM. Regulation of cellular interactions with laminin by integrin cytoplasmic domains: A and B structural variants of the a6b1 integrin differentially modulate the adhesive strength, morphology and migration of macrophages. *Mol Cell Biol* (1994) 5:679–90. doi: 10.1091/mbc.5.6.679
35. Thomas-Ecker S, Lindecke A, Hatzmann W, Kaltschmidt C, Zanker KS, Dittmar T. Alteration in the gene expression pattern of primary monocytes after adhesion to endothelial cells. *Proc Natl Acad Sci USA* (2007) 104 (13):5539–44. doi: 10.1073/pnas.0700732104
36. Zigmond E, Jung S. Intestinal macrophages: well educated exceptions from the rule. *Trends Immunol* (2013) 34(4):162–8. doi: 10.1016/j.it.2013.02.001
37. Arango Duque G, Descoteaux A. Macrophage cytokines: involvement in immunity and infectious diseases. *Front Immunol* (2014) 5:491. doi: 10.3389/fimmu.2014.00491
38. Takada Y, Hisamatsu T, Kamada N, Kitazume MT, Honda H, Oshima Y, et al. Monocyte chemoattractant protein-1 contributes to gut homeostasis and intestinal inflammation by composition of IL-10-producing regulatory macrophage subset. *J Immunol* (2010) 184(5):2671–6. doi: 10.4049/jimmunol.0804012
39. Bain CC, Mowat AM. The monocyte-macrophage axis in the intestine. *Cell Immunol* (2014) 291(1-2):41–8. doi: 10.1016/j.cellimm.2014.03.012
40. Randolph GJ, Beaulieu S, Lebecque S, Steinman RM, Muller WA. Differentiation of monocytes into dendritic cells in a model of transendothelial trafficking. *Science* (1998) 282(5388):480–3. doi: 10.1126/science.282.5388.480
41. Fleger-Weckmann A, Ustun Y, Kloepper J, Paus R, Bloch W, Chen ZL, et al. Deletion of the epidermis derived laminin gamma1 chain leads to defects in the regulation of late hair morphogenesis. *Matrix Biol* (2016) 56:42–56. doi: 10.1016/j.matbio.2016.05.002
42. Frieser M, Nockel H, Pausch F, Roder C, Hahn A, Deutzmann R, et al. Cloning of the mouse laminin alpha 4 cDNA. Expression in a subset of endothelium. *Eur J Biochem* (1997) 246(3):727–35. doi: 10.1111/j.1432-1033.1997.t01-1-00727.x
43. Schuler F, Sorokin LM. Expression of laminin isoforms in mouse myogenic cells in vitro and in vivo. *J Cell Sci* (1995) 108(12):3795–805.
44. Sorokin LM, Pausch F, Frieser M, Kroger S, Ohage E, Deutzmann R. Developmental regulation of the laminin alpha5 chain suggests a role in epithelial and endothelial cell maturation. *Dev Biol* (1997) 189(2):285–300. doi: 10.1006/dbio.1997.8668
45. Woodfin A, Voisin MB, Beyrau M, Colom B, Caille D, Diapouli FM, et al. The junctional adhesion molecule JAM-C regulates polarized transendothelial migration of neutrophils in vivo. *Nat Immunol* (2011) 12(8):761–9. doi: 10.1038/ni.2062
46. Schenkel AR, Mamdouh Z, Chen X, Liebman RM, Muller WA. CD99 plays a major role in the migration of monocytes through endothelial junctions. *Nat Immunol* (2002) 3(2):143–50. doi: 10.1038/ni749
47. Liao F, Huynh HK, Eiroa A, Greene T, Polizzi E, Muller WA. Migration of monocytes across endothelium and passage through extracellular matrix involve separate molecular domains of PECAM-1. *J Exp Med* (1995) 182 (5):1337–43. doi: 10.1084/jem.182.5.1337
48. Bixel G, Kloep S, Butz S, Petri B, Engelhardt B, Vestweber D. Mouse CD99 participates in T-cell recruitment into inflamed skin. *Blood* (2004) 104 (10):3205–13. doi: 10.1182/blood-2004-03-1184
49. Samus M, Seelige R, Schafer K, Sorokin L, Vestweber D. CD99L2 deficiency inhibits leukocyte entry into the central nervous system and ameliorates neuroinflammation. *J Leukoc Biol* (2018) 104(4):787–97. doi: 10.1002/JLB.1A0617-228R
50. Prieto J, Eklund A, Patarroyo M. Regulated expression of integrins and other adhesion molecules during differentiation of monocytes into macrophages. *Cell Immunol* (1994) 156(1):191–211. doi: 10.1006/cimm.1994.1164
51. Ammon C, Meyer SP, Schwarzfischer L, Krause SW, Andreesen R, Kreutz M. Comparative analysis of integrin expression on monocyte-derived macrophages and monocyte-derived dendritic cells. *Immunology* (2000) 100 (3):364–9. doi: 10.1046/j.1365-2567.2000.00056.x
52. Fujiwara H, Kikkawa Y, Sanzen N, Sekiguchi K. Purification and characterization of human laminin-8. Laminin-8 stimulates cell adhesion and migration through alpha3beta1 and alpha6beta1 integrins. *J Biol Chem* (2001) 276(20):17550–8. doi: 10.1074/jbc.M010155200
53. Jakubzick CV, Randolph GJ, Henson PM. Monocyte differentiation and antigen-presenting functions. *Nat Rev Immunol* (2017) 17(6):349–62. doi: 10.1038/nri.2017.28
54. Hanley PJ, Xu Y, Kronlage M, Grobe K, Schon P, Song J, et al. Motorized RhoGAP myosin IXb (Myo9b) controls cell shape and motility. *Proc Natl Acad Sci USA* (2010) 107(27):12145–50. doi: 10.1073/pnas.0911986107

Conflict of Interest: The authors declare that the research was conducted in the absence of any commercial or financial relationships that could be construed as a potential conflict of interest.